Submission to Sensors and Diagnostics

Portable Microfluidic Immunoassay Platform for Detection of Inflammatory Protein Biomarkers

Gihoon Choi[1], Betty B. Mangadu[1], Yooli K. Light[2], and Robert J. Meagher[2], *

[1] Sandia National Laboratories, Biotechnology & Bioengineering Dept., Livermore, CA, USA

[2] Sandia National Laboratories, Systems Biology Dept., Livermore, CA, USA

* Corresponding Author, Email: rmeaghe@sandia.gov

Table of Contents

Microfluidic chip fabrication using a reusable 3D-printed mold

For reliable in-house microfluidic chip manufacturing, we implemented 3D-printing of soft lithography mold for polydimethylsiloxane (PDMS)-based devices. Figure S2A depicts the entire microfluidic device fabrication process. Briefly, the chip layout was designed and printed using a CAD design tool (Solidworks) and a 3D printer (Form 3). The print was sonicated with IPA for 10 min to remove uncured resin, then incubated in a UV box at 60 °C for 30 min. The cured print surface was treated with oxygen plasma for 2 min, then silane-modified. It has been reported that residual catalysts and monomers in photopolymer resin interfere with the polymerization of PDMS where it is in contact with the mold surface, disrupting the covalent bonding between PDMS and glass substrate. Therefore, a thin protective coating on the mold surface has been considered, such as ink airbrushing[1] or methacrylate monomer resin[2]. We created a hydrophobic barrier using 1H,1H,2H,2H-Perfluorodecyltrichlorosilane to avoid the PDMS uncuring. Besides, a hydrophobic surface helps ensure the mechanical stability of a high aspect-ratio microchannel (e.g., 0.5 x 1 x 2.75 mm^3) by making the peel-off step easier. After PDMS casting, reagent loading inlets were punched. Finally, patterned PDMS and glass surface were activated by oxygen plasma and then irreversibly bonded using a custom-design alignment tool (Figure S2B and C).

Comparison of washing performance between 1D and 2D agitation

We performed the CRP detection assay in the microfluidic immunoassay platform to compare the washing performance between 1D and 2D washing. Two sets of 0 ng/mL CRP samples were incubated with capture beads and detector agents, then a subsequent washing step was performed (Figure S3A). We varied the washing methods by incorporating either 1D- or 2D-agitation in EM-sequence (Figure S3B). The number of washing cylces, washing chamber geometry, and total washing volumes loaded in the chamber were set to identical for both washing methods. To quantify the washing performance, we compared the CL signal generated from 0 ng/mL CRP samples immediately after washing. Figure S3C depicts a threefold higher CL signal from the sample set prepared by 1D washing sequence compared to the 2D washing sequence. This indicates that 2D agitation outperforms 1D agitation in rinsing unbound detector antibodies from the sample chamber. This is because the carryovers around the bead clump smears out along a line in 1D wash, whereas it smears out over a square in 2D wash. In other words, the diffusion of the carryovers from the bead clump to the bulk occurs more rapidly with 2D agitation than with 1D

agitation. While a narrow and elongated chamber design in 1D washing can decrease the characteristic time for the diffusion of the contaminants by reducing the diffusion length (i.e., the average distance from channel side wall to the center of bead clump), it requires a longer channel length to hold sufficient washing volume. In contrast, 2D agitation capability offers more flexibility in microfluidic chamber design.

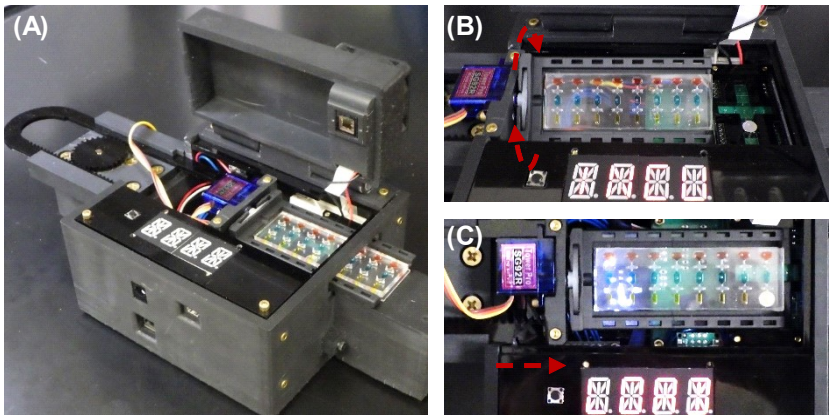

Supplementary Figure S1. Photo of fully assembled microfluidic immunoassay platform. (A) The lid is opened to show the inside of the platform during the operation for the demonstration purpose. (B) The chip tray tumbles back and forth in vertical direction (arrow) by servo motion. (C) As chip tray moves to right by rack and pinion mechanism (arrow), each testing unit in test chip aligned with electromagnetic array.

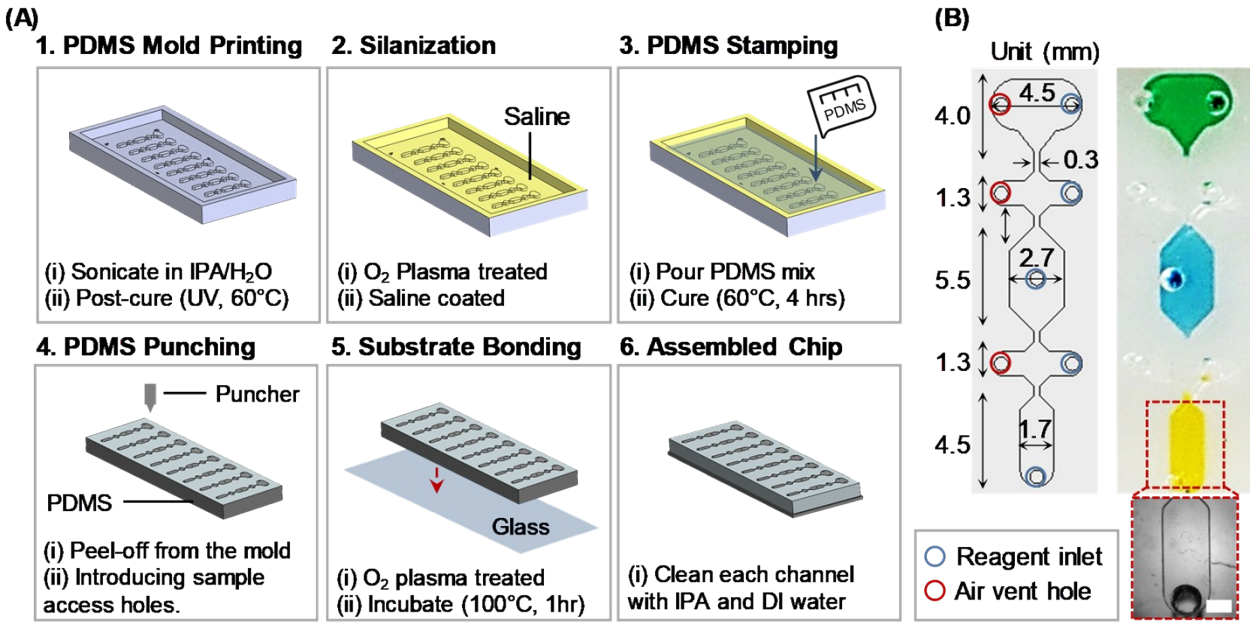

Supplementary Figure S2. Microfluidic chip fabrication. (A) Schematic of step-by-step fabrication process. (B) Schematic of microfluidic chip with detailed channel dimensions (left panel). Channel height is 1 mm. Photo image of the microfluidic chip (right panel). Color dye is loaded for visualization. The reagents are filled from bottom to top chambers (yellow, blue, then green). Then, valving chamber is filled from right to left. Vent holes are patterned to remove air bubbles while loading the reagents and mineral oil. Microscope image of the microfluidic channel after PDMS-glass bonding (Scale bar: 1 mm). The assembled microfluidic device showed tight sealing for liquid and well-defined channel edges.

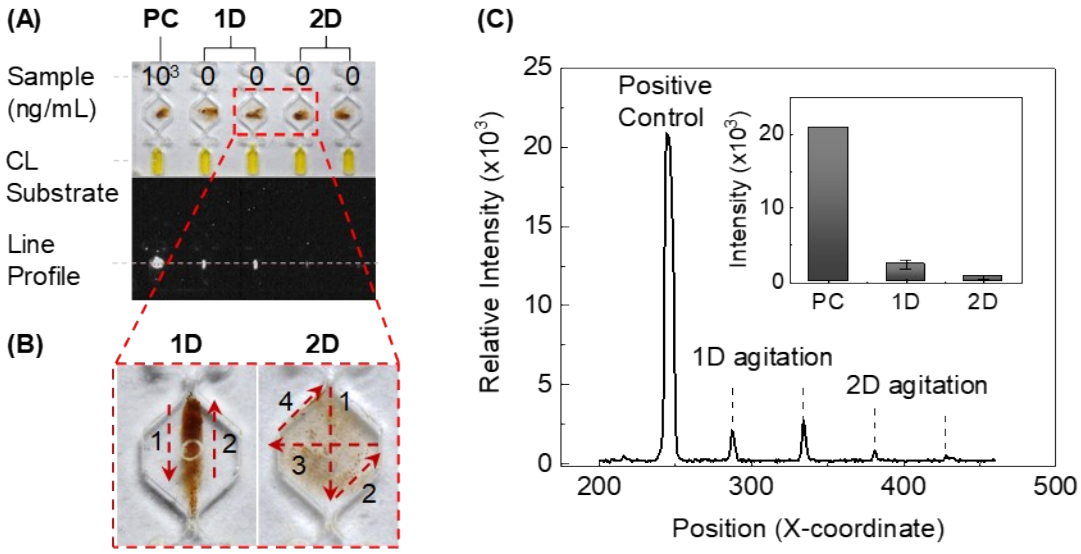

Supplementary Figure S3. Comparison of 1D-, 2D-agitation washing performance. (A) Microfluidic chip image used for comparison tests. Immunoassay tests were performed using 10^3 and 0 ng/mL CRP samples. 0 ng/mL CRP samples were washed differently by 1D- or 2D-agitation sequence. The positive control (PC) with a concentration of 10^3 ng/mL confirms the functionality of the reagents, validating that the assay performs as intended. The grayscale chip image displays chemiluminescence (CL) intensities from the test samples. (B) Photo image of washing chambers illustrating the distinct 1D and 2D mixing patterns. Magnetic beads were dispersed along the magnet actuation path. 2D magnet actuation is beneficial in dispersing the bead clump in multiple directions, while 1D actuation is limited to two directions. (C) The plot showed the line profile (dotted lines) extracted from the grayscale image. The bar plot (subset) clearly demonstrates the significant difference in CL signal between 1D and 2D agitation. The average and standard deviation were derived from the peak intensity values.

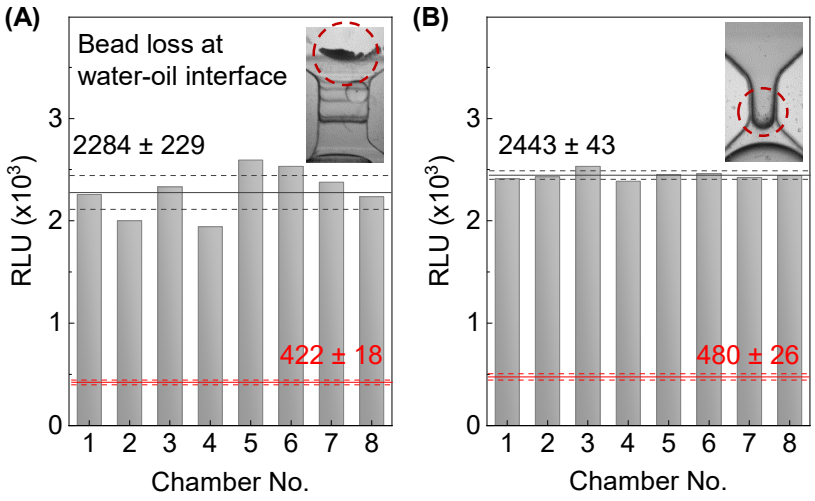

Supplementary Figure S4. Uniformity of magnetic beads extraction at water-oil interface. HRP-labeled bead aliquots were loaded into eight testing units. The wide water-oil interface showed significant CL signal variation (A), whereas the narrow interface showed excellent consistency (B). Insets are end-point microscope images of the magnetic beads remaining after the bead extraction process.

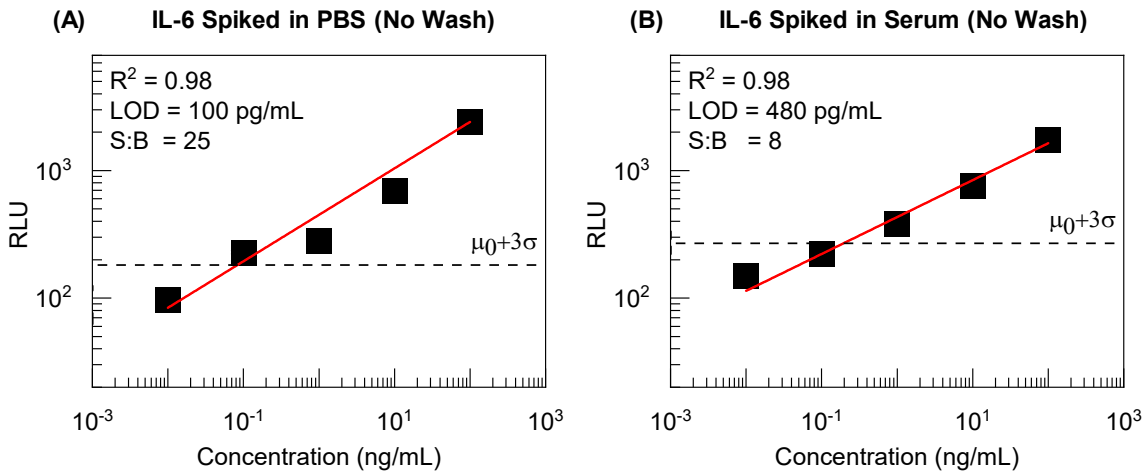

Supplementary Figure S5. Sensitivity results without incorporating the washing steps. An order of magnitude higher detection limit (i.e., 480 pg/mL) and significantly decreased signal-to-background ratios (S:B) were observed for PBS and complex serum samples compared to the washing incorporated sensitivity results (LOD = 10 pg/mL, S:B = 56, see Figure 6E). A comparison of three standard curves, including Figure 6E confirmed that the source of background is indeed a carry-over from unbound HRP-labelled detector antibodies from the sample chamber.

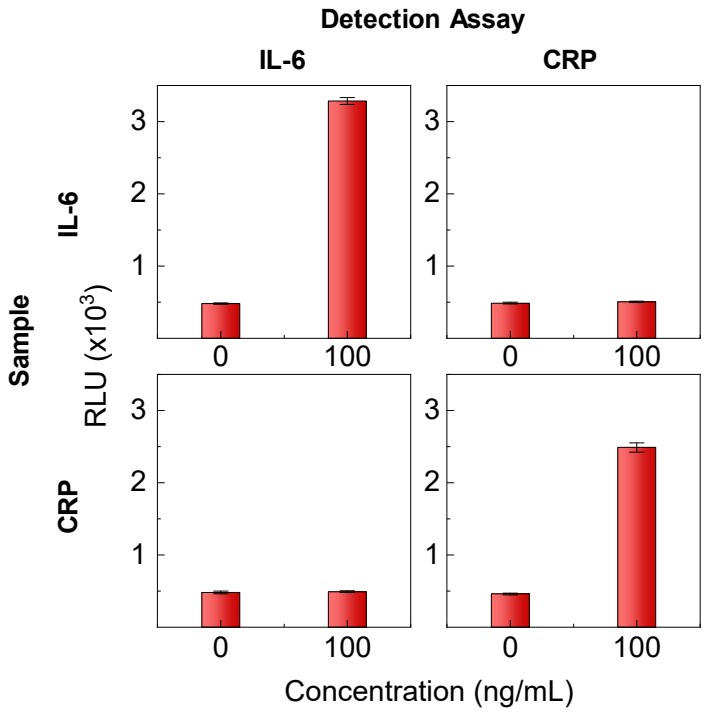

Supplementary Figure S6. Cross-reactivity test results using two inflammation biomarkers. 0 and 100 ng/mL IL-6 and CPR were spiked in PBS for the test. The corresponding detection assay only picked up the positive samples, confirming the target-specific capability without cross-reactivity.

Reference

1. G. Comina, A. Suska and D. Filippini, *Lab Chip*, 2014, **14**, 424-430.
2. S. Razavi Bazaz, N. Kashaninejad, S. Azadi, K. Patel, M. Asadnia, D. Jin and M. Ebrahimi Warkiani, *Advanced materials technologies*, 2019, **4**, 1900425.